Journal Pre-proof

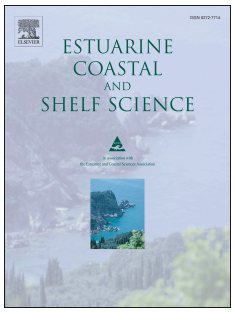

Modern sedimentary facies in a progradational barrier-spit system: Goro lagoon, Po delta, Italy

Annelore bezzi, Giulia Casagrande, Davide Martinucci, Simone Pillon, Carlo Del Grande, Giorgio Fontolan

PII: S0272-7714(19)30152-0

DOI: https://doi.org/10.1016/j.ecss.2019.106323

Reference: YECSS 106323

To appear in: *Estuarine, Coastal and Shelf Science*

Received Date: 15 February 2019

Revised Date: 18 June 2019

Accepted Date: 2 August 2019

Please cite this article as: bezzi, A., Casagrande, G., Martinucci, D., Pillon, S., Del Grande, C., Fontolan, G., Modern sedimentary facies in a progradational barrier-spit system: Goro lagoon, Po delta, Italy, *Estuarine, Coastal and Shelf Science* (2019), doi: https://doi.org/10.1016/j.ecss.2019.106323.

Modern sedimentary facies in a progradational barrier-spit system: Goro lagoon, Po delta, Italy

Abstract

Barriers and spits connected to fluvial sedimentary sources represent environments which tend to evolve rapidly and experience sudden transformations, mainly driven by changes in sediment supply and path. As a consequence, the variability of facies is significant even within small sedimentary records. The 7 km long barrier-spit system facing the Goro Lagoon, and fed by the mouth of the Po di Goro, is a typical example of an accretionary coastal morphotype, suitable to describe contiguous nearshore depositional environments and their stratigraphic signatures, variability, and relationships. Thirteen short cores of sediment were sampled in order to represent the variable depositional sub-environments from the shoreface (prodelta-delta front) to the back barrier, crossing the active barrier-spit and the ancient spit arms and relative swales. The description of the modern sedimentary records, improved upon using core X-rays, has been coupled with information on the morphological changes which occurred during the period of maximum spit development (1955-2000), based on available aerial photos and a cartographic / topographic dataset. The results obtained allow for the description and interpretation of the depositional environments changing at the human-scale. Sediments of the upper shoreface are quite uniform, composed by evenly laminated sands; the transition between delta front and prodelta at a depth of 6 m is marked by the alternation of sand and mud beds. These reflect the periodic changes in sediment supply by the river, as well as storm events. The most recent spit branch and the relative back barrier-swale environment are the result of the rapid progradation of the spit system, which implies phases of rapid longshore growth, hooked spit development, cannibalization, overwash, and breaching. Morphodynamic changes have resulted in an overlap of short sedimentary records where stratigraphic signatures are linked either to phases of sediment transport and selection by waves and tidal currents (cross-bedding, foreset and planar laminated sands, shell imbrication,

massive beds) or to phases of sedimentary stasis when biological activity is predominant (algal mat and bioturbation). Human signature is also well marked inside the stratigraphic record. Clam harvesting is carried out within the lagoon causing the physical disturbance and winnowing of the superficial sediment, thus inducing the local formation of graded beds and shell rehash.

Keywords: modern facies; stratigraphy; barrier island; spit; sediment dynamics; progradation

1. Introduction

The study of sedimentary sequences and the analysis of facies are of considerable importance in reconstructing the environmental contexts and transformations that have occurred over time. In highly dynamic environments with sudden transformations, the variability of facies is significant, even within very small thicknesses, as in the case of coastal areas with a high rate of sedimentation. This is the case of barrier systems connected to fluvially derived point sources of sediment, such as delta systems and their related interdistributary bays (Anthony et al., 2014; Anthony, 2015).

Changes in solid load, primarily, could induce rapid changes in the physiography and evolutionary styles of deltas (Elliott, 1986a; Suter, 1994; Rubin et al., 2015). Consequently, the prevalence of fluvial or coastal processes determines various delta regimes (wave or river dominated) according to the Galloway model (1975). Over time, different regimes may induce alternate phases of erosion and deposition. These processes could affect the entire or portions of the delta - i.e., through delta lobe switching (Correggiari et al., 2005a; 2005b) - as well as its related coastal morphologies.

Dynamic equilibrium between fluvial supply, longshore drift, and subsidence affects primarily deltaic barrier systems, inducing progradational or transgressive phases and diverse geomorphic responses (McBride et al., 1995; McBride and Byrnes, 1997; Anthony and Blivi, 1999; Simeoni et al., 2007).

Deltaic coastlines are particularly prone to responding to human-made forcing factors, which influence depositional environments at the human scale and determine a co-evolution process (Welch et al., 2017). River damming, embankments, and sand mining on the river-bed contribute to the modification of the sedimentary fluxes from rivers to the sea (Anthony, 2015; Rubin et al., 2015; Otvos, 2018; Ritchie et al., 2018). Human-induced subsidence may exacerbate the relative sea level rise thus increasing flood risk (Antonioli et al., 2017) as well as the accommodation space, responsible for submergence and drowning potential of barrier systems (Sanders and Kumar, 1975; De Falco et al., 2015).

Although a large number of the world's barrier islands are undergoing a transgressive evolutionary trend (Bird, 1985; FitzGerald et al., 2018), deltaic barrier systems could represent the exception, when aggradation or progradation occurs in association with a high sediment supply (Hayes and Ruby, 1994; Morton, 1994; Garrison et al., 2010).

Progradation processes promote the contiguity and simultaneous occurrence of various depositional environments in relatively little space and time. On the shoreface, wave action and sedimentation by river suspended load assume a dominant role according to different river phases (Elliott 1986a; Suter, 1994). Longshore currents and wave swash are responsible for spit progradation with different rates and mechanisms of berm accretion (Hine, 1979). At the same time, depressions between newly formed barriers determine the segregation of swales (Otvos, 2000), unavoidably involved in tidal circulation near tidal inlets (FitzGerald, 1988), and enclosed cat's eye ponds (Otvos, 2000; Davis et al., 2003). Storm surge may produce dune erosion, berm overtopping and washover breach (Leatherman et al., 1977; Orford and Carter, 1982; Héquette and Ruz, 1991). Washover can evolve by processes of channel fill or fan deposition and subsequent salt marsh colonization (Elliott, 1986b; Rodriguez et al., 2018).

Such types of depositional environments have been mostly studied in terms of stratigraphy and the reconstruction of depositional models during the Holocene (Davis et al., 2003; Hein et al., 2013;

Gonzales –Villanueva et al., 2015; Forde et al., 2015; Fruergaard et al., 2015; Raff et al., 2018), whereas analyses of small scale variability is less common. These analyses could be useful to further the understanding of the changing role of coastal forcing in space and time (Clarke et al., 2014).

After the Nile, the Po River has the largest delta in the Mediterranean (Got et al., 1985), as the consequence of extremely rapid growth over the last 500 years, within the framework of a well-documented history and close interaction between natural and anthropogenic forcing factors (Correggiari et al., 2005a; Simeoni and Corbau, 2009). Despite a generalized transgressive phase during the 20th century due to anthropogenic subsidence and riverbed excavation, a fast-progradational spit system developed in the southernmost part of the Po delta, between the delta front of the Po di Goro River and the Goro Lagoon (Dal Cin, 1983; Simeoni et al., 2007).

This branched barrier-spit system is particularly well-suited to allow for a detailed study on nearshore modern depositional and human-influenced environments in a progradational context and their stratigraphic markers, based on short sediment cores.

The aim of the study is to describe the depositional facies as well as their spatio-temporal variability and to interpret macroscopic and radiographic evidence in terms of coastal evolution as seen by a direct verification of the environmental conditions in aero-photogrammetric and topographical surveys.

The intention of the work is to investigate the possibility that signatures and stratigraphic sequences are preserved and therefore recognizable as “event-related” in the sub-environments typical of a barrier - spit system.

2. Study area

The Goro lagoon is the southernmost of the lagoons of the Po delta and covers over 20 km², with an average depth of 1.5 m (Fig. 1).

A set of studies have described the characteristics of the lagoon and relative barriers and their origin and evolution (Simeoni ed., 2000). They are closely linked to the development and evolution of the Po delta, in particular to the sedimentary load and constructive contribution of the Po di Goro distributary arm (Simeoni et al., 2000; Fontolan et al., 2000), also testified to by the wide submerged prodelta depositional body, the *Goro-Gnocca lobe* (Correggiari et al., 2005a). Less important is the input coming from the south, responsible for the formation of the Volano spit (Fontolan et al., 2000). Tide is semidiurnal with a mean range of 60 cm (40 cm during neap tide and 120 cm during spring tide) (Simeoni et al., 2007).

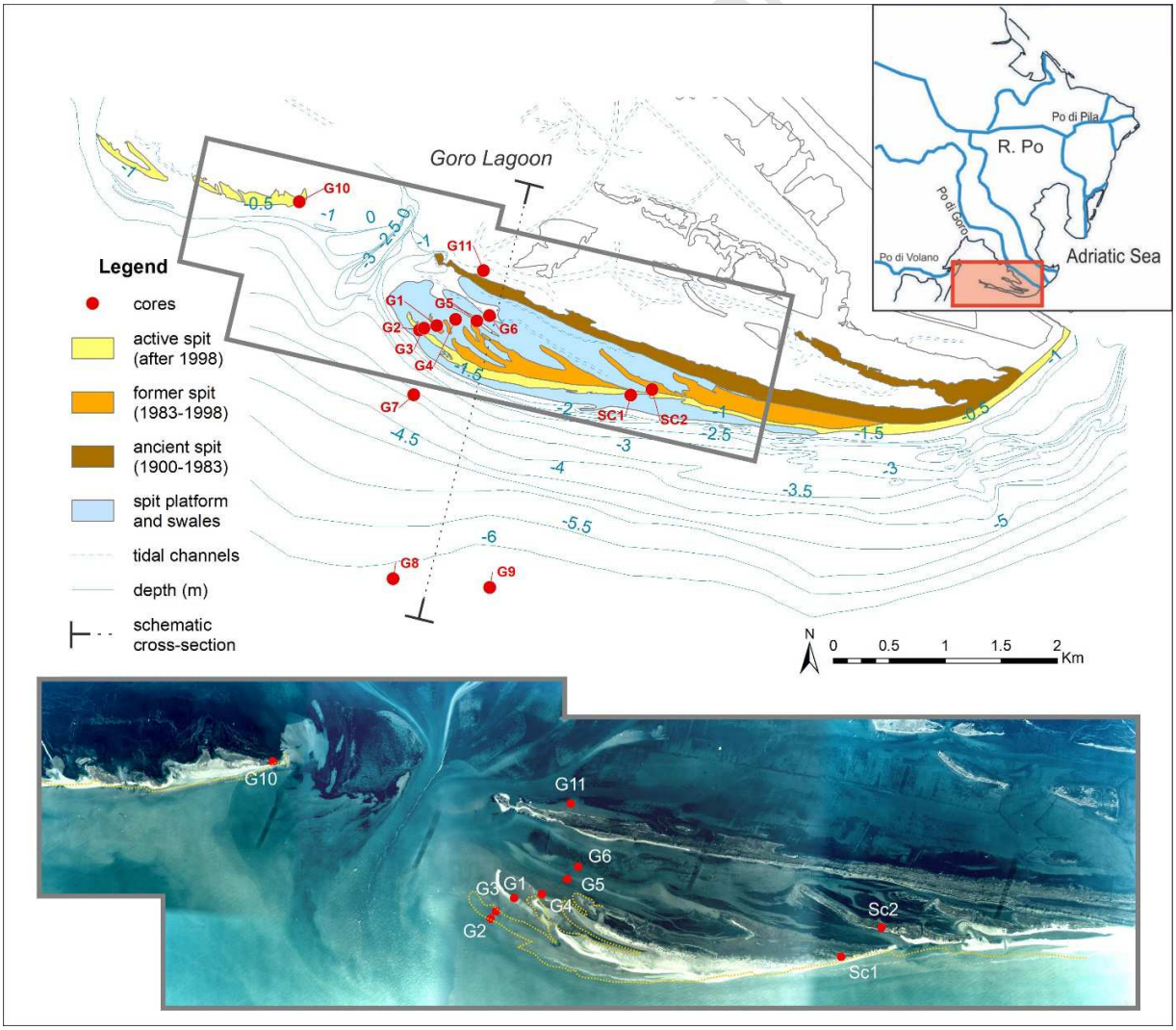

Fig.1 – Location and a simplified geomorphological map of the study area (upper part) with sediment core positions. Aerial photographs collected in winter 1998 (with the shoreline from 2000 superimposed in yellow) offer the best view of the subaerial and intertidal environments (lower part). The cross section indicated on the map is represented in Fig.3.

During the last century, strong anthropogenic pressure in the area was caused by reclamation and land use modifications in the fluvial basin, and by coastal management works (Simeoni et al., 2007). Moreover, since 1986, a large part of the Goro lagoon, as well as some sectors of its coastal area, has been intensely exploited for the seeding, cultivation, and harvesting of *Tapes philippinarum* clams (Manila clam), currently one of the pillars of the local economy (Bartoli et al., 2016). Like the entire delta the Goro area is subject to a thorough subsidence due to both natural (sediment compaction, eustatism, etc.) and anthropogenic factors (groundwater withdrawal, onshore, and offshore gas extraction). Land subsidence during the last century was dramatic, accounting for an average cumulative value of more than 1.5 m, with a peak of more than 3 m in the inner part of the delta (Corbau et al., 2019). The phenomenon occurred mainly from 1950 to 1957, due to extensive withdrawals of methane-rich groundwaters, with maximum rates up to 250 mm/yr, i.e., one hundred times higher than the natural long term subsidence rate. After groundwater withdrawal stopped in 1960, subsidence progressively decreased, from values of ca. 65 mm/yr in 1957-67, ca. 18-28 mm/yr during 1967-74, up to 5-11 mm/yr after 2002 (Corbau et al., 2019).

Despite the progressive decrease in the fluvial sediment load between 1940 and 1980, the lagoon has always acted as a "sedimentary trap" and the lagoon - barrier system has maintained a positive sediment budget (Simeoni et al., 2000).

The suspended load of the Po is responsible for stable prodelta deposits in the area facing the Goro mouth and the Goro lagoon as recognized by Correggiari et al., (2005a). The front-prodelta transition boundary can be identified at a depth which varies from 4 m (in the area of the Volano inlet) to 7-8 m (in the area of the mouth of the Goro) based on the seasonal analysis of the sediments done by Bortoluzzi et al., (1984). This boundary is confirmed by the textural transition from sandy mud to mud indicated in the sedimentological map made by Brambati et al., (1988). Fine sediment can enter the lagoon and deposit on the bed in the inner part (Dal Cin and Pambianchi, 1991), determining infilling processes (Simeoni et al., 2000).

The sandy bed load is distributed southwards by longshore currents, also partially supplied by the inputs from the northern river branches between Po di Pila and Goro. It constitutes the entire area of the barrier-spit system (Simeoni et al., 2000) and indicates the dominance of coastal processes with higher energy, affecting the southernmost tip of the Po delta, due to the bimodal wave regime from NE and SE (Ruol et al., 2018). In fact, wind direction is primarily from NE (8.4 m/s) secondarily from SE (6.8 m/s) (Calderoni, 1982; Ruol et al., 2018). The prevalent direction of the waves is from 60° to 120° and energy is relatively small. Low energy waves (significant height, Hs<0.5 m, period T=3 s) are the most frequent (68%); medium energy waves (Hs=0.5-1.5 m, T=3-6 s) make up 12.7% of the total, storm waves (Hs>1.5 m T=5-8s) and extreme waves (Hs= 4.5 m) are represented only by frequencies of 2% and 0.5%, respectively (Simeoni et al., 2007).

Simeoni et al. (2007) reconstructed the history of the Goro barrier-spit system for the period from 1870 to 2000, using historical maps, topographical maps, aerial photographs, and satellite images. According to the authors, since the end of the 19th century, a progradational process resulted in a series of parallel spits, formed through various morphological stages, mainly influenced by the interaction between natural and anthropogenic forcing factors and the relative dominance of fluvial or marine processes over time.

Fig. 2 presents the main phases of spit evolution in 1955, 1981/83, 1996 (Simeoni et al., 2007) and 2000 (Del Grande et al., 2001), detected by mapping on aerial photographs or by DGPS surveys. At the end of the first period (1955-1981/83), the main spit lengthened westward up to 2.7 km and the eastward part of the spit prograded seaward. During the second period (1986-1996), a new spit arm formed seaward in the central part of the main spit, characterized by a *branched growth* ascribable to a reduction in the fluvial sedimentary load and a subsequent wave domain phase. The progressive westward lengthening of the spit was interrupted by the opening of an artificial secondary inlet (in 1989), 2 km east of the western apex. This intervention aimed to enhance the water exchange of the lagoon. As a consequence, the development of a new ebb-tidal delta enlarged the spit platform updrift, thus favoring the development of new spit arms seawards; the contemporary effect was the starvation of the remnant western spit, isolated downdrift as a barrier island.

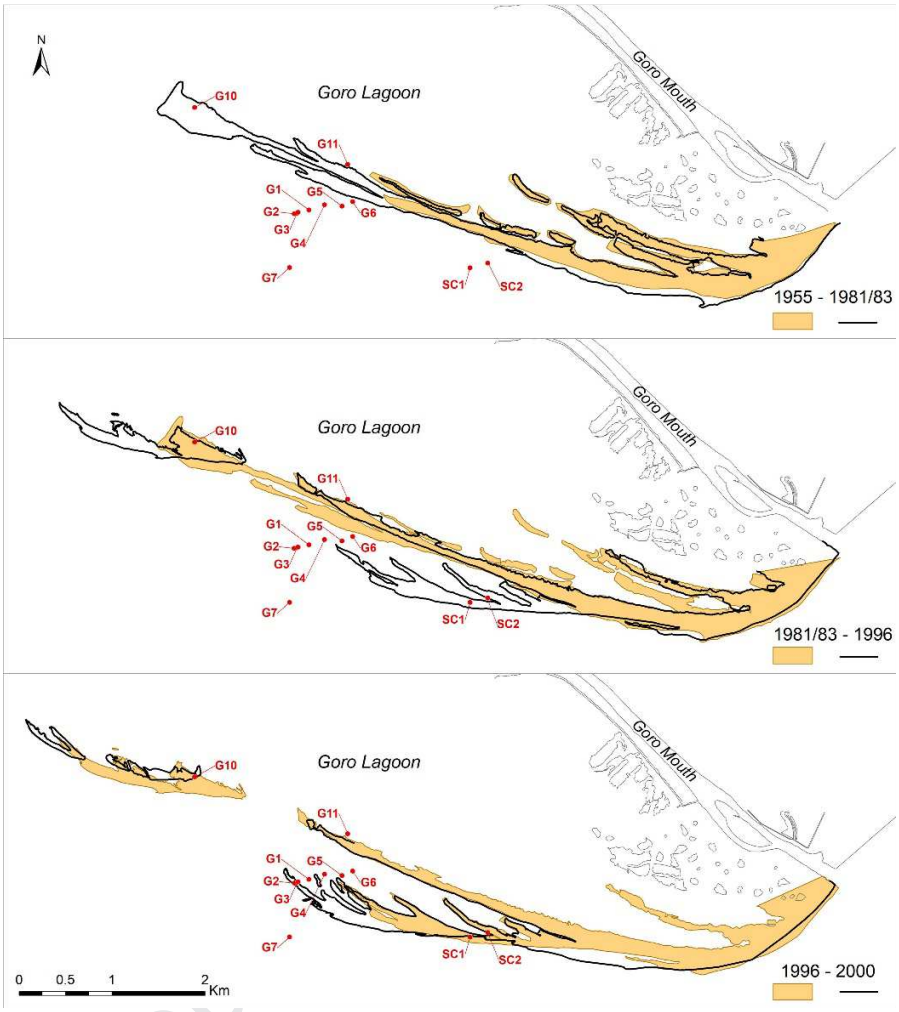

157

158 Fig.2 – Evolution of the Goro barrier-spit system from 1955 to 2000. The shoreline dataset is adapted
159 from Simeoni et al. (2007) and Del Grande et al. (2001).

160

161 The subsequent evolution based on aerial photographs from 1996 and the shoreline survey from 2000,
162 corresponding to the situation at the time core samples were taken, shows the development of an
163 additional spit branch. At the same time, the erosion and the landward migration of the residual barrier
164 island between the two inlets occurred due to the sediment starvation generated by the artificial inlet
165 opening and its subsequent development.

3. Materials and methods

In June 2000, during the most rapid phase of the spit system development, 13 sediment cores were sampled. The cores were taken manually with cylindrical PVC pipes of variable diameter (from 8 to 10 cm) inserted in the sediment (with a penetration depth from 21 to 99 cm) on several coastal morphologies. All cores were geo-referenced with a GPS and at each sampling site, the characteristics of the depositional environment were annotated and described thanks to field observations and aerial photographs from 1998. The evolutionary context was reconstructed according to the data from Simeoni et al. (2007) and Del Grande et al. (2001) consisting of the digitized shoreline from 1955, 1981-83, 1986, 1988, 1996, 1998, 1999 and 2000 obtained from various sources (regional cartography, aerial photographs, and GPS surveys).

Cores were sectioned, photographed and then described macroscopically. The description includes grain size, color (evaluated by comparison using the Munsell® Soil Color Charts, Edition 2000), degree of homogeneity and hydration, texture, the presence of sedimentary structures, biogenic content (shells or plant remains), activity (bioturbation), and accumulation of organic matter.

In the post-cutting phase, one of the two hemicylinders was radiographed to increase the possibility of recognizing sedimentary structures, lithological changes, organic-rich beds, shells and shell hash. The X-ray source used is a unidirectional generator Balteau Baltospot GFD 200/8. The selected exposure time was 25 s for an amperage of 5 mAs and a voltage of 95 kV.

In the next phase, the radiographs were digitally enhanced and converted to positive grayscale; when necessary, the brightness, contrast, and intensity were balanced, and finally, the 3D shadow relief effect was used to highlight the dominant features and to enhance the visualization of sedimentary structures.

As far as the description of the sedimentary facies is concerned, the sampling technique (manual) allows one to obtain short but continuous cores with minimal sediment deformation. At the same time, X-ray analysis allows for the recognition of structures not evident to the naked eye.

4. Results

The spit - barrier system of Goro was sampled with a series of short cores which allow for the typifying of different contemporary depositional environments. Core location is presented in Fig. 1, as well as in Fig. 2, where the core position is related to the morphological changes from 1955-2000.

Core logs were grouped according to the present depositional environments as follows: shoreface (delta front and prodelta), active spit, back barrier (Fig. 3). According to the evolutionary phases depicted in Fig. 1, the back barrier includes the initial spit, active up to 1981-83, hereinafter referred to as the "ancient spit", and "former spit", corresponding to a set of ridges developed and progressively abandoned during the spit progradation which occurred after 1981-83 and before the development of the contemporary (2000) "active spit" arm.

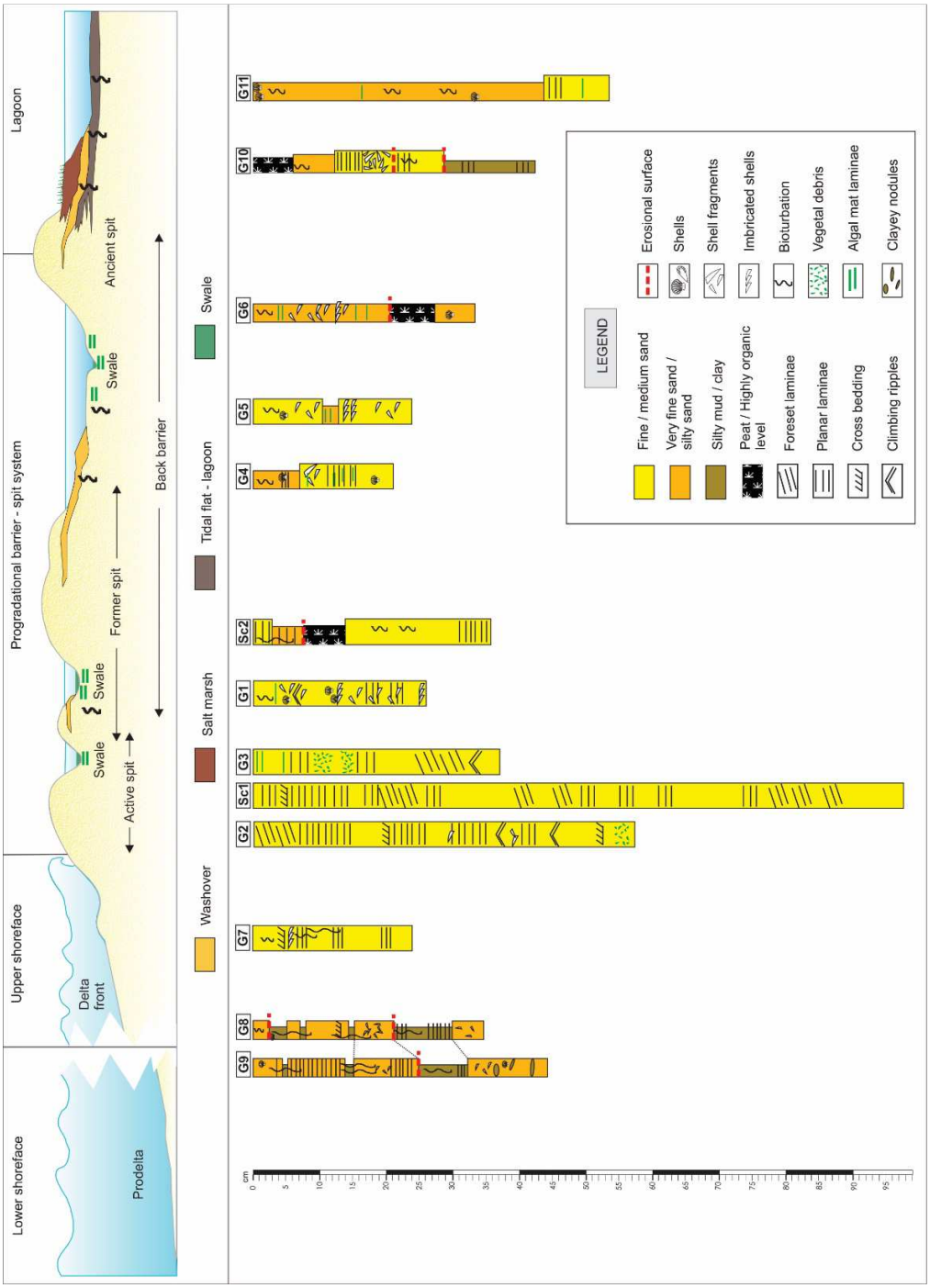

202

203 Fig.3 – Schematic cross-section of the barrier-spit system with depositional environments and

204 representation of relative core logs. See Fig. 1 for the position of the section.

205

Three cores were collected in the deltaic shoreface facing the Goro lagoon at the western limit of the Po di Goro lobe: G7 was taken at a depth of -4.2 m in a distal portion of the delta front, G8, and G9 at -6 m and -6.20 m, respectively, at the limit between the delta front and upper prodelta.

Core G7 consists of fine sand with weak laminations, identifiable only via X-ray, olive (5Y 5/3) or olive gray (5Y 5/2) in the most surficial layers, darker at the bottom (very dark gray 5Y 3/1). Planar lamination, cross-bedding and an imbricated shell level are visible only via X-ray. Muddy flocs are present and responsible for a mottled aspect that masks lamination. Bioturbations are scarce and limited to the top level. G8 and G9, collected at ca. -6.0 m depth, present the interbedding of coarser levels (above mm) of very fine sand or silty sand and finer muddy beds. Sand is often laminated with planar beds or climbing ripples. Erosional surfaces are evident on the bottom of some sandy beds and shell hash or clayey nodules mixing in the sandy beds are present (bottom of G9). Bioturbation involves the first 30 cm of both cores, on the top of G8 a bed truncates some vertical burrows. The two cores can be correlated due to the presence of a sharp erosional surface in the middle part of the record and some lithological/structural similarities (Fig. 3).

Cores G2, G3, and Sc1 were sampled on the active spit surface (within 1 m above mean sea level). In particular, core Sc1 on the beach berm of the “former spit” in a tract with an evident erosional scarp, where the sedimentary sequence was naturally exposed. Cores G2 and G3 were sampled on the western terminal lobe of the “active spit”, on the beach face, and on the near back barrier, respectively. The cores consist entirely of light sand (olive gray 5Y 5/2, olive 5Y 5/3, grayish brown 2,5Y 5/2, light brownish gray 2,5Y 6/2) with horizontal or sloped flat planar laminations. Sand is only occasionally massive and, in some cases, there are cross-bedding and climbing ripples, identified only by X-ray. In core G3, algal mats are easily recognizable on the top and as an underlying lamina transparent on X-rays (white in positive). Beds with a high content of vegetal debris can be distinguished either by a macroscopic darker shade of

229 olive color or by less dense (lighter shade) and granular appearance on X-rays. Finally, whole shells were

230 found in both G2 and G3.

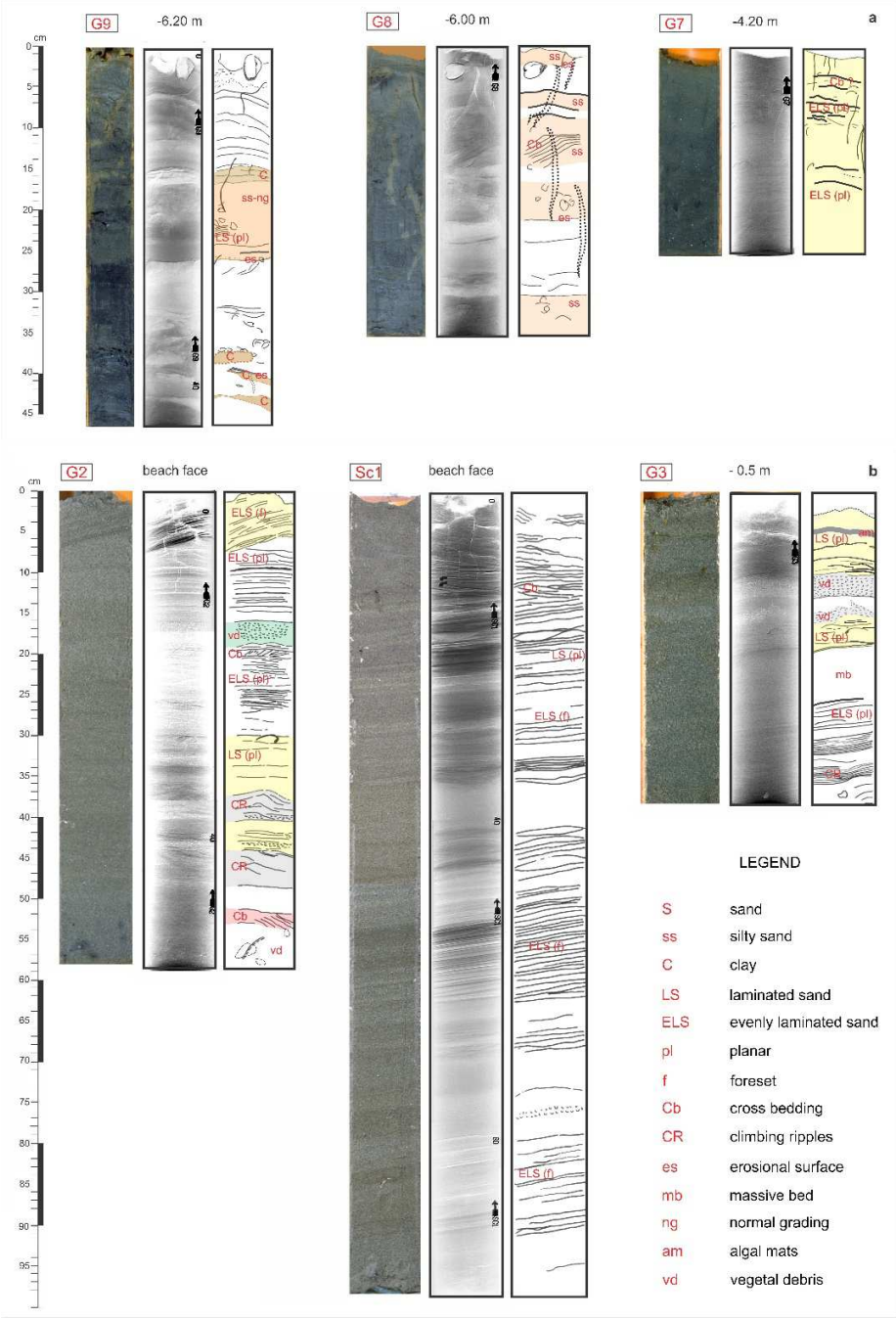

231

Fig.4 – Detail of cores collected on the shoreface (prodelta-delta front) (a) and active spit (b). Each core is represented by a photograph, an X-ray (positive) and a schematic interpretation, i.e., major sedimentary structures, bioturbations and shells. Color background is used to depict homogeneous bed characteristics due to lithology or sedimentary structures, identified by the acronyms in the legend. The name of the core and sampling depth are reported at the top of each core triplet.

In the back barrier area, six cores were sampled. G1 and SC2 represent modern back barrier conditions in areas previously involved in active sedimentation and then isolated by the rapid growth of a new spit seaward (1998-2000). In particular, G1 was sampled on a spit formed between 1996 and 1998, partially eroded and fragmented by waves between 1998 and 2000. The remnants were then fronted seaward by a newly formed spit arm, and became a low energy environment where sedimentation was influenced by marginal tidal circulation connected to the nearby tidal inlet and by occasional overwash involving the external barrier. SC2 was sampled on the western flank of a branch of the “former spit”, which was formed between 1986 and 1988 in the central part of the spit system. Core G4 was taken from a protected environment with only weak tidal currents on the back barrier of the northernmost branch of the “former spit” developed between 1996 and 1998. Cores G5 and G6 were sampled on the side of the largest back barrier swale, connected to the artificial Goro inlet and dominated by tidal currents. Core G11 was sampled from the backside of the ancient spit. Between 1955 and 1981-83, the area experienced a rapid transition from open bay to back barrier, because of the formation of the new spit arms. Finally, core G10 was taken from the western part of the artificial Goro inlet, in an area subjected to rapid and dramatic environmental deterioration. The initial back barrier environment (1986-1996) underwent flooding processes due to the erosion of the barrier after the artificial opening of the secondary Goro inlet (1989).

The back barrier cores show a limited facies variability (Fig. 5): the most represented sediment tails are fine sand, very fine sand or silty sand, but beds of medium sand (G5) and silty mud (G10) are still present locally. Sediment color is generally dark (dark olive gray 5Y 3/2, dark grayish brown 2,5Y 4/2, dark gray 5Y 4/1, very dark gray 2,5Y 3/0, black 2,5Y 2/0) with frequent superficial lighter thin layers, because of oxidation processes. Sands are weakly laminated (G1), laminated (G4, G10, G11, Sc2) or massive (G1), with tractive structures as climbing ripples (G1). In three cases (SC2, G6, and G10) levels of peat or highly organic levels, respectively, are evident, derived from plant remains and seen as completely transparent on the X-rays (white in positive). Bioturbation structures are common, both superficial and buried. There are algal mats as laminae or levels, quite evident on the X-ray (white in positive) and beds with shells, whole or in fragments, sometimes arranged in imbricate levels. Graded beds, very rich in shell fragments arranged without a preferential orientation of the valves, are present in core G4.

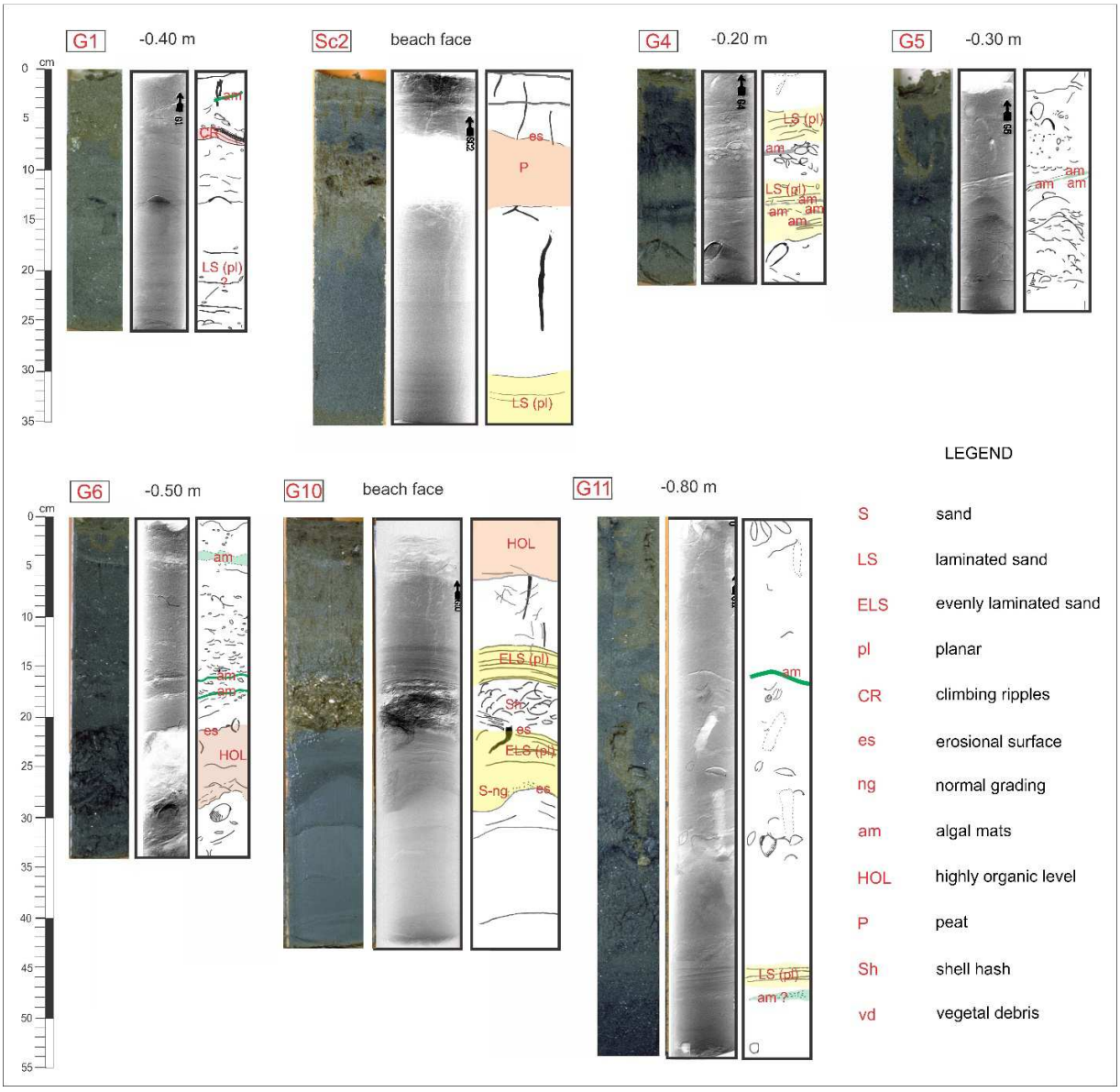

273

274 Fig.5 – Detail of cores collected on the back barrier and swale. Each core is represented by a
275 photograph, an X-ray (positive) and a schematic interpretation, i.e., major sedimentary structures,
276 bioturbations, and shells. Pale colors or alternate blank areas are used to depict homogeneous bed
277 characteristics due to lithology or sedimentary structures, identified by the acronyms in the legend. The
278 name of the core and sampling depth are reported at the top of each triplet.

279

5. INTERPRETATION AND DISCUSSION

The morphological and physical characteristics of present depositional environments (delta front and prodelta, active spit, back barrier) and their recent morpho-evolution reconstructed according to cartographic and topographical data, allow for the interpretation of core facies and their sequence.

5.1 Shoreface (delta front-prodelta transition)

Delta front and prodelta represent contiguous transitional environments where bedload transport by waves or fine fluvial suspended load, respectively, prevails. Within the upper shoreface the prevalent wave-induced transport of the sandy sediments induces weak laminations, cross-bedding arrangement, and bioclast imbrication (core G7). At the same time, the mottled macroscopic appearance is due to the presence of muddy inclusions, which were likely deposited in the form of flocculated aggregates, settled from the river hypopycnal plume (Nittrouer et al., 2004). The area of influence of the turbid plume of the different tributaries of the Po River is quite large, and asymmetrically distributed southwards, thus involving the entire area facing the Goro spit, as seen by the plume dispersal captured by satellite during the prevailing local wind forcing (Braga et al., 2017; Manzo et al., 2018). This implies a markedly asymmetrical distribution of the whole delta sediment, as already highlighted by Brambati et al. (1988).

The sedimentological alternation (visible in cores GB and G9) interpreted as a coarsely interlayered bedding (CIB) structure (Reineck and Singh, 1980), reflects periodic changes in sediment supply and turbid emission by the river, associated with alternating events of normal discharge and floods. As observed by Nittrouer et al. (2004) the sediment released to the Adriatic Sea by the Po River consists of more than 90 percent mud, composed of silt and clay particles, the latter significantly flocculated along the lower river course. The high concentration of flocculated sediment leads to rapid settling on the

shoreface, and mud deposits begin to form in the Adriatic at water depths of 4 to 6 m, which can be considered the closure depth or the limit between the delta front and prodelta.

The CIB structure in the cores confirms the above-described environmental conditions, which begin to be conservative for cohesive deposits right here, although still subordinate to the coarser non-cohesive component. Coarser beds, composed of very fine sand, are clearly identifiable on the X-rays (positive) by their marked dark color, and predominate in the sampled series, demonstrating the effective exposure to north-easterly and easterly winds. Thus, the wave-induced drift processes are responsible for the selection of the sand component driven westward.

Occasionally the coarser levels present some typical characteristics of storm layers or of sands swept by wave action, such as an erosive base which truncates bioturbation, and cross-bedding. Storm beds in the modern sedimentary record of the wave-dominated continental shelf are common, also at depths greater than 60 m (Budillon et al., 2005). In the northern Adriatic, the wave regime is significantly low since the basin physiography constrains it, but south-easterly and especially north-easterly winds can produce waves which have a significant impact on sedimentation. Waves can easily reach orbital bottom velocity up to 40 cm/s in the Po prodelta at -12 m depth (Nittrouer et al., 2004), thus inferring significantly higher values in the upper-mid shoreface. The winnowing of the sea bottom by a high energy event was quite effective at producing a chaotic mixing of sand, fragments, and bivalve shells in the lowermost part of core G9. The original interlayered muddy beds were also involved in re-working and mixing, and were subsequently re-arranged as residual mud drapes, aggregates, or lenticular nodules.

Differences in bed thickness and the lack of continuity of some beds in a relatively limited space (G8 and G9 cores were collected 1 km apart) can be explained if taking into consideration the crenulated distribution of the local shoreface sediments, as reported by Simeoni et al. (2000). Investigations in the

same area (Correggiari et al., 2005b) highlighted the presence of a rhythmic pattern of sand waves or subaqueous transverse bars (sensu Niedoroda and Tanner, 1970 and Pellon et al., 2014) better classifiable as long finger bars (Falques et al., 2018), which are likely responsible for the irregular distribution of the sandy sedimentary drapes following the same pattern. Even though a specific investigation is currently ongoing by other Authors, the presence of persistent long finger bars, accomplished by shoreline undulations, could be linked to the so-called high-angle wave mechanism (Falques et al., 2017), possibly due to the high angle of the refracted waves from east and northeast, which also drives the spit morphodynamics and the river plume dispersal.

5.2 Active spit

The present depositional environment of the sandy active spit is part of the branched system formed between 1983 and 2000 and described by Simeoni et al. (2007) as a result of the wave domain and the high efficiency of longshore drift supplied by the mouth of the Po di Goro.

The sampled series (Sc1, G2, and G3) can be considered illustrative of various mechanisms of berm development in distinct portions of the spit, each causing the beach to be prograde at different rates, as suggested by Hine (1979). According to Hine's model, along with the straight portion of the spit (Fig. 6 section AA'), periods of low energy conditions promote the small accumulation of sediment on the beach face. The resulting structure of the beach face is evident in the sequence of core Sc1: plane stratification dipping seaward with an angle of 10-14°. Upward, a bed of coarser sand, arranged in a horizontally planar stratification, corresponds to an increase in energy and water level, which resulted in the redistribution of sediments on the top of the main berm (berm overtopping). Further to the west where the spit begins to curve, nearshore longshore bars characterize the spit platform and, during calm conditions (fair weather conditions), tend to migrate through the low tide terrace and weld onto the beach berm, resulting in a process of berm accretion (Hine, 1979; Jensen et al., 2009). The progradation

is fastest nearest to the tip of the curved spit (Fig. 6, section BB'), and a process of berm-ridge development occurs (Hine, 1979). The rapid buildup of stacked berm-ridges (beach ridges in more modern terminology) isolates original runnels that remain inactive and protected from wave action and tidal current. The resultant beach pond can be filled slowly by wind-transported sand or evolve into a high intertidal swale (Otvos, 2000).

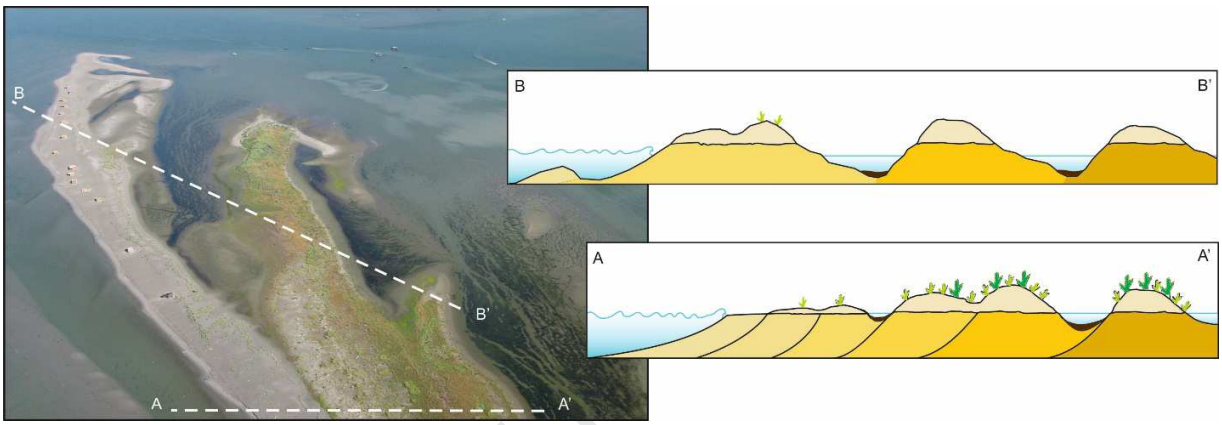

Fig.6 – Application of Hine's model (1979) of berm-ridge growth and beach development to the study area. On the left, the view from above the active Goro spit; on the right the different examples of the form sequences of a progradational spit: profile AA' shows the scheme of longshore bars welded onto beach berm, and profile BB' shows the tip of the spit characterized by berm-ridges and swales, (photo credit: Ferrara Province).

These mechanisms of berm development and beach progradation can explain the sedimentary structure of cores G2 and G3 (Fig. 4b). In fact, the foreset structure on the top of G2 corresponds to the beach face lamination during the growth phase. According to observations made by Hine (1979) and Jensen et al. (2009) the evenly planar laminae standing above the foreset can represent the topset of the berm, built up during overtopping in high tide conditions. The preservation of interbedding of planar laminated sands and levels with climbing ripples or cross-bedding in the lower half of core G2 (18-55cm) indicates an environment of deposition under the mean sea level (i.e., sub-tidal or lower inter-tidal) with rapid

sediment accumulation. It appears in agreement with the progressive emersion phase of the longshore bars. On the bottom, small dark stains linked to organic remains coupled with bioturbation identify a phase of scarce sediment supply, likely associated with the first phase of longshore bar construction. The planar laminated sand alternating with massive beds in the middle and at the bottom of core G3 represent phases of transport by weak tidal currents interrupted by overtopping events, able to accumulate more massive and coarser beds.

The proliferation of algal or microbial mats, as in the uppermost part of core G3, highlights the temporary establishment of protected conditions. In general, mats benefit from low-rate sedimentation but occasionally become buried by the landward-directed sedimentation of storm sands (Gerdes, 2007). In detail, beds with a high level of vegetal debris content, distinguished at 15 cm and 12 cm from the top, are attributed to filamentous mats embedded with or mixed with sand. According to Gerdes (2007), this structure indicates pioneer transient stages of non-deposition, suffering subsequent sediment burial. A longer period of sedimentary stasis favors the establishment of a mature microbial mat, as the lamina observed at 5 cm from the top of G3, as well as the coherent mat cover at the topmost of the core (Fig. 7). This could be used as a further marker of a progradational spit, which causes changes from active sedimentation on the berm-ridge to a low-energy organic-bearing context typical of the swale.

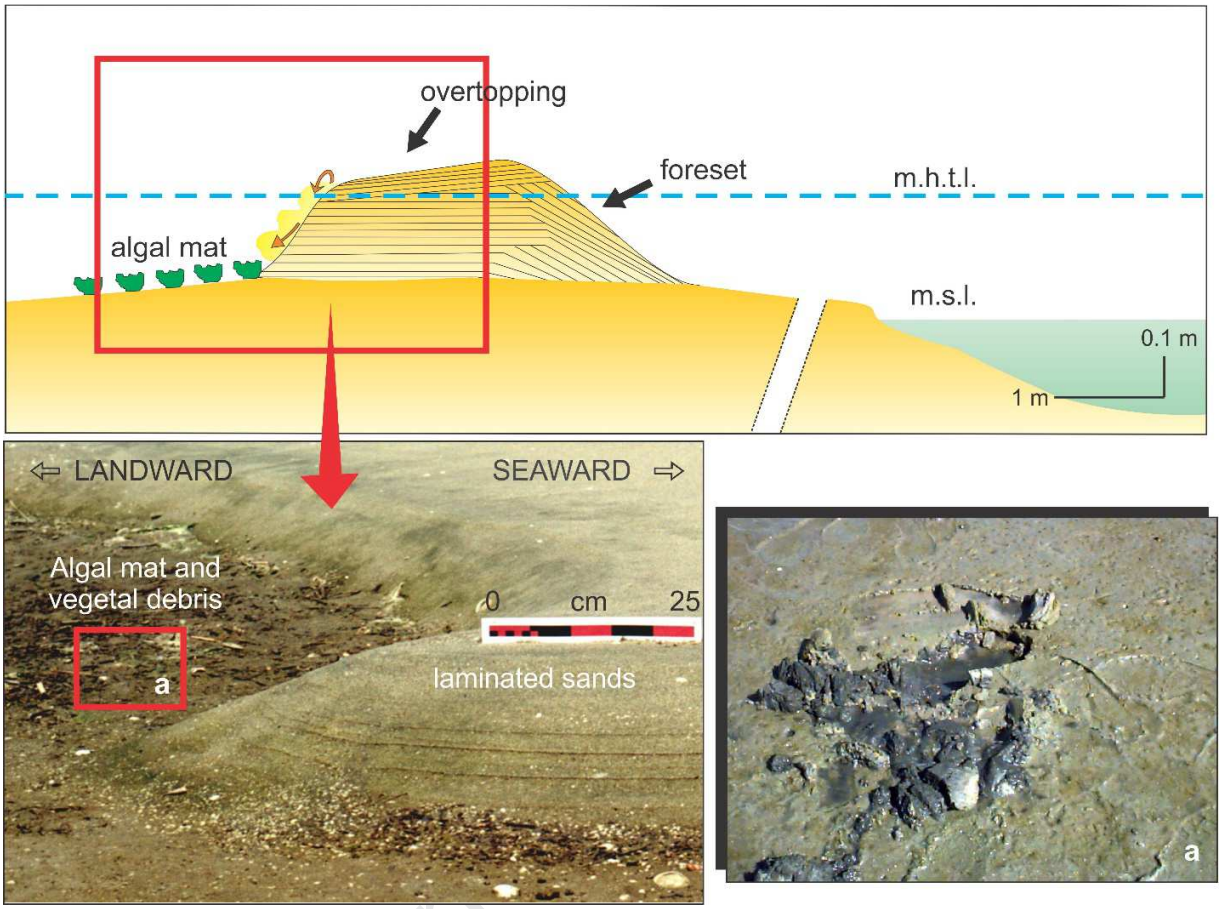

385

386 Fig.7 – Schematic representation of sampling site G3, consisting of an active spit arm with relative
387 macroscopic facies (e.g., algal mat and laminated sands).

388

389 **5.3 Back barrier and swale**

390 The rapid formation and evolution of the branched spit system, as documented by shoreline data,
391 isolated the back barrier and swale environments, where local characteristics are related to the
392 temporary prevalence of different coastal processes.

393 The area proximal to the "former spit" apex (core G1) testifies to the alternation of a different process
394 domain in the wider progradational context. Weakly laminated structures and levels of imbricated,
395 mostly whole shells with concavity downward are indicators of the efficiency of tidal currents in

sediment transport in the first phase. Upwards in the sequence, a set of climbing ripples indicates a more recent phase of sedimentary input, likely associated with overwash processes. The wave-reworking hypothesis is supported by the presence of a level very rich in shells (bivalves) and of a massive sandy bed on the top of the core. The burrows (bioturbation) and biomat laminae indicate the modern, calmer environment and a reduction in sediment input.

On the eastern part of the spit branch formed between 1986 and 1988, the first phase of spit construction is in evidence at a low depth (35 cm). A sand unit with planar lamination at the bottom of core SC2 represents the topset of the berm, according to the previously mentioned process (cfr. active spit). The intense bioturbation, visible in the central part of the sequence, can be attributed to a decrease in longshore sediment supply after the formation of the new spit seawards. The protected conditions allows for the formation of a salt marsh (peat level) overlaid through erosional contact by a bed of laminated silty sand and sandy layers, testifying to the recovery of the deposition after an erosional event. The abrupt sedimentary shift from peat to a higher energy silty-sand phase can be explained by taking into consideration a breach formation in the thin tract of the seaward spit (captured in aerial photos in the winter of 1998, see Fig. 1), that allowed for the reactivation of circulation in the swale channel between the two spit branches. The breach was already closed two years later, thus implying that the subsequent sedimentary stasis enhanced the diffuse superficial bioturbation.

In the swale area, sediment reworking is widespread due to clam harvesting in shallow waters and results in bed furrows, as visible in Fig. 8. Beds of artificial reworked sediment are present at different depths in the sampled core (G4), and are overlaid by tractive laminae and thin layers of sandy silt and algal mat. These attest to a swale environment, where natural sedimentation of fine suspended sediment is dominant at times and where, during stasis conditions, microbial mats develop above the lagoon bed.

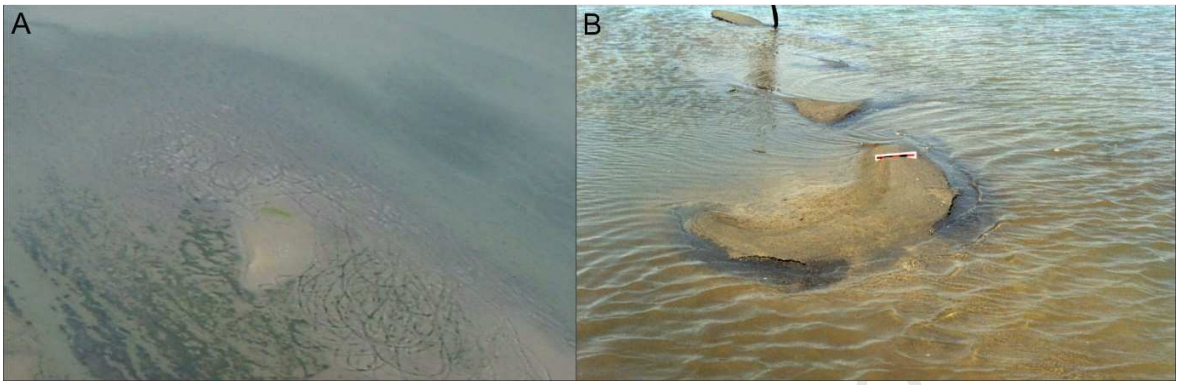

Fig.8 –Effects of the physical disturbance caused by boats used for clam harvesting in the Goro Lagoon (a) aerial view with circular tracks left by fishing boats (photo credit: Ferrara Province); (b) detail of the furrows (benchmark length 25 cm).

At the swale connected to the artificial Goro inlet, the variable intensity and effects of tidal currents enhanced or hindered sedimentation, according to the progressive migration of the active spit branches facing seaward. The two series G5 and G6 represent this type of depositional environment. Lagoon infill processes are represented by levels of imbricate shells and relatively coarser sand on the bottom part of G5; they are a consequence of barrier overwash linked to its former proximity to the active spit. Reduced circulation and sedimentary stasis are marked by the microbial mats or by fine sediment deposition, as well as by a highly organic level, present in the middle of G5 and the lower part of core G6. The diffuse high amount of bivalve shells, whole or fragmented, should be seen as the results of intensive activity of clam cultivation and harvesting in the areas adjacent to the tidal inlet. In some cases, the tractive action of tidal current allows for the formation of imbricated shell beds, typical of tidal channels (Davis et al., 2003).

The backside of the “ancient spit” (G11) is dominated by sand with a high quantity of shells, despite the relatively high distance from the current shoreline. This indicates the permanence of transgressive

coastal processes, in particular overtopping and overwash, as evidenced by the presence of weak lamination, partially destroyed by heavy and scattered active burrowing. The dark color indicates the partial preservation of the organic component, and the presence of algal mat layers or laminae indicates temporary phases of sedimentary quiescence, typical of areas partially protected from tidal circulation and waves.

A typical transgressive sequence is seen in core G10, where the predominantly clayey material on the bottom is topped by a sandy layer via an erosive surface. This coarser level is normally graded in the lower part and thinly laminated in the upper one. The transgressive sequence ends with a marked washover deposit, consisting of an irregular bed of shells immersed in a sandy matrix. Washover occurs when during storm events, waves bypass or break up the barriers, depositing the material transported in the form of a delta originating from unidirectional intermittent waves (Schwartz, 1982). Usually, these are graded at the base, with abundant shell lag levels, and laminated on the top, due to the subsequent re-arrangement by swash (topset laminae). Finally, the top of the core maintains a small back barrier regressive sequence, as seen by a layer of bioturbated silty sand (tidal flat deposits) overlaid by organic mud, rich in salt marsh plant remains (roots and leaves).

5.4 Remarks on modern progradational barrier spit facies

High resolution stratigraphy derived by short core data coupled with the diachronic information on environmental changes which occurred during the progradational phases of the barrier spit system provides a detailed new insight and a thorough understanding of the sedimentary architecture linked to the complex morphodynamics of human-altered deltaic coastlines.

A schematized regressive barrier, which occurs when the rate of sediment accumulation exceeds the rate of the creation of sediment accommodation (Timmons et al., 2010), implies that the shoreline prograde seaward, through a large scale welding of the migrating barrier bodies. A detailed analysis of

460 the morphological evolution of the Goro barrier spit system during the maximum progradational phase,
461 highlights the placement of a succession of detached sand bodies which occupy the former spit
462 platform, thus creating a complex system of low-lying ridges and swales. The changes in the pattern of
463 the longshore drift due to human activities (mostly linked to the control of the river sediment supply,
464 and opening of new tidal inlets) condition the growth of the spit system. The result is an irregular
465 process, which implies phases of rapid longshore growth, hooked spit development, cannibalization,
466 overwashing and breaching (Simeoni et al., 2007). The correspondent sedimentary sequences present
467 an overlap of short records, each associated both temporally and spatially to a distinct event or
468 environmental transformation.

469 The dominance of sand in almost all the cores is a consequence of the high rate of progradation of the
470 spit system, therefore the abandoned spit branches preserve the sandy characteristics of frontal
471 barriers. Signatures of the new position in a more protected environment are diffuse bioturbation and
472 laminae or beds of algal mat and the typical dark color of the sediments due to poor oxygenation. If the
473 protected conditions persist over time and the bed elevation is adequate, the sandy levels may be
474 interspersed with peat beds, as a result of colonization by intertidal superior vegetation evolving into a
475 salt marsh. Alternatively, the more protected areas can become traps of fine (mainly silt) material,
476 coming from either the river plumes or from the re-suspension induced by clam harvesting. The
477 concomitant effect of subsidence and the high rate of progradation favor the low elevation of the
478 barriers and spits and small scale overtopping or breaching processes are thus frequent. Stratigraphic
479 recognition of small transgressive processes - better considered reactivation processes - is common in
480 the areas close to the barrier, because of occasional overtopping or washover events resulting in
481 massive beds of coarser material rich in shells. Transgressive signals are particularly effective in the most
482 starved portions of the spit system, where longshore sediment supply is impeded, resulting in a short
483 negative sequence as a consequence of human activity, i.e., the artificial opening of a tidal inlet.

The strong human influence on alongshore drift and subsequent hybrid (regressive and transgressive) evolutionary behavior of barrier systems (Anthony and Blivi, 1999), as well as the effects of re-suspension induced by the man-made physical disturbance of the sea-bottom, are factors to be taken into account in studies on contemporary (Anthropocene) stratigraphy.

6. Conclusion

The Goro spit is a typical example of a deltaic barrier-spit whose evolutionary style is the direct result of the transformation of the territory and the changing discharge regime of the Po River. The progressive reduction of fluvial sediment supply during the last century modified the evolutionary styles of the spit without yet changing the overall progradational trend. The persistent progradation of the spit between 1955 and 2000 is emblematic of a human-influenced process that cannot be summarized by a simple stratigraphic scheme. Thanks to the particular characteristics of this spit barrier system, a series of contiguous nearshore depositional environments occur and evolve at the human scale.

Coupling the recent detailed stratigraphy with contemporary high-resolution data on shoreline changes represents the methodological approach, which allows for an improvement in the interpretation of facies and related processes. At the same time, X-ray analysis on the sediment cores increase the possibility of recognizing sedimentary structures originating from small-scale changes of the different depositional environments.

The data allow for a series of main, contiguous, depositional sub-environments to be identified, with a relatively high facies variability and sedimentary signatures. The accurate reconstruction of the coastal evolution implies the recognition of either long-lasting periods or abrupt events responsible for the environmental changes involving portions of the spit that can induce shifting from a high to a low energy environment, as well as sporadic trend reversal. The results and corresponding interpretation increase

knowledge regarding the sedimentary characteristics of the Po region and represent a contribution to understanding a depositional model of barrier islands, in particular when human activities are crucial in determining longshore transport changes and, consequently, the coexistence of different evolutionary trends.

Appendix A. Supplementary data

Funding

This research was previously carried out with financial support from the Agriculture Department of the Emilia Romagna Region (Objective 5B, Subprogram 1, Measure 7), and MIUR Cofin98 research funds. The dataset review and new investigation were funded by the Flagship Project RITMARE – The Italian Research for the Sea – coordinated by the Italian National Research Council and funded by the Italian Ministry of Education, University and Research within the National Research Program 2011-2013.

Declarations of interest

None

Acknowledgements

We would like to acknowledge S. Bencivelli, G. Gabbianelli, U. Simeoni, U. Tessari, A. Zamariolo and the crew of the vessel Hydra provided by the Province of Ferrara, for the support given for authorizations, logistics, and for help during surveys and sampling.

528 **References**

529 Anthony, E.J., 2015. Wave influence in the construction, shaping and destruction of river deltas: A
530 review. Marine Geology 361, 53-78. https://doi.org/10.1016/j.margeo.2014.12.004

531 Anthony, E.J., Blivi, A.B., 1999. Morphosedimentary evolution of a delta-sourced, drift-aligned sand
532 barrier–lagoon complex, western Bight of Benin. Marine Geology 158, 161–176.
533 https://doi.org/10.1016/S0025-3227(98)00170-4

534 Anthony, E.J., Marriner, N., Morhange, C., 2014. Human influence and the changing geomorphology of
535 Mediterranean deltas and coasts over the last 6000 years: from progradation to destruction phase?
536 Earth Science Reviews 139, 336-361. https://doi.org/10.1016/j.earscirev.2014.10.003

537 Antonioli, F., Anzidei, M., Amorosi, A., Lo Presti, V., Mastronuzzi, G., Deiana, G., De Falco, G., Fontana, A.,
538 Fontolan, G., Lisco, S., Marsico, A., Moretti, M., Orrù, P.E., Serpelloni, E., Sannino, G.M., Vecchio, A.,
539 2017. Sea-level rise and potential drowning of the Italian coastal plains: flooding risk scenarios for 2100.
540 Quaternary Science Reviews 158: 29-43. https://doi.org/10.1016/j.quascirev.2016.12.021

541 Bartoli, M., Castaldelli, G., Nizzoli, D., Fano, E.A., Viaroli, P., 2016. Manila clam introduction in the Sacca
542 di Goro lagoon (northern Italy): ecological implications. Bullettin of Japan Fisheries Research and
543 Education Agency 42, 43-52.

544 Bird, E.C.F., 1985. Coastline changes. A global review. Wiley, Chichester, 219 p.

545 Bortoluzzi, G., Frascari, F., Ravaioli, M., 1984. Ricerche sedimentologiche in aree marine adriatiche e
546 tirreniche finalizzate alla comprensione dei fenomeni di inquinamento costiero. Memorie della Società
547 Geologica Italiana 27, 499-525.

548 Braga, F., Zaggia, L., Bellafiore, D., Bresciani, M., Giardino, C., Lorenzetti, G., Maicu, F., Manzo, C.,
549 Riminucci, F., Ravaioli, M., Brando, V.E., 2017. Mapping turbidity patterns in the Po river prodelta using
550 multi-temporal Landsat 8 imagery. Estuarine, Coastal and Shelf Science 198, 555-567.
551 https://doi.org/10.1016/j.ecss.2016.11.003

552 Brambati, A., Ciabatti, M., Fanzutti, G.P., Marabini, F., Marocco, R., 1988. Carta sedimentologica
553 dell'Adriatico settentrionale. CNR, Istituto Geografico De Agostini, Novara.

554 Budillon, F., Violante, C., Conforti, A., Esposito, E., Insinga D., Iorio M., Porfido S., 2005. Event beds in the
555 recent prodelta stratigraphic record of the small flood-prone Bonea Stream (Amalfi Coast, Southern
556 Italy). Marine Geology 222–223, 419– 441. https://doi.org/10.1016/j.margeo.2005.06.013

557 Calderoni, G., 1982. Regime anemologico nel Delta del Po alla foce dell'Adige. Annali dell'Università di
558 Ferrara, sez. IX, Scienze Geologiche e Paleontologiche vol. VIII n. 4, 61–69.

559 Clarke, D.W., Boyle, J.F., Chiverrell, R.C., Lariob, J., Plater A.J., 2014. A sediment record of barrier estuary
560 behaviour at the mesoscale: interpreting high-resolution particle size analysis. Geomorphology 221, 51-
561 68. http://dx.doi.org/10.1016/j.geomorph.2014.05.029

562 Corbau, C., Simeoni, U., Zoccarato, C., Mantovani, G., Teatini, P., 2019. Coupling land use evolution and
563 subsidence in the Po Delta, Italy: revising the past occurrence and prospecting the future management
564 challenges. Science of The Total Environment 654, 1196-1208.
565 https://doi.org/10.1016/j.scitotenv.2018.11.104

566 Correggiari, A., Cattaneo, A., Trincardi, F., 2005a. The modern Po Delta system: lobe switching and
567 asymmetric prodelta growth. Marine Geology 222-223, 49-74.
568 https://doi.org/10.1016/j.margeo.2005.06.039

569 Correggiari, A., Cattaneo, A., Trincardi, F., 2005b. Depositional patterns in the Late Holocene Po Delta
570 system. In Giosan, L., Bhattacharya, J.P. (Eds.), River Deltas–Concepts, Models, and Examples Society for
571 Sedimentary Geology, Special pubblication 83, pp. 365–392. https://doi.org/10.2110/pec.05.83.0365

572 Dal Cin, R., 1983. I litorali del delta del Po e alle foci dell'Adige e del Brenta: caratteri tessiturali e
573 dispersione dei sedimenti, cause dell'arretramento e previsioni sull'evoluzione futura. Bollettino Società
574 Geologica Italiana 102, 9-56.

575 Dal Cin, R., Pambianchi, P., 1991. I sedimenti della Sacca di Goro (Delta del Po). In: Bencivelli, S. and
576 Castaldi, N. (Eds.) Studio Integrato sull'Ecologia della Sacca di Goro. Provincia di Ferrara, Franco Angeli,
577 Milano: 253-263.

578 Davis, R.A.Jr., Yale, K.E., Pekala, J.M., Hamilton, M.V., 2003. Barrier island stratigraphy and Holocene
579 history of west-central Florida. Marine Geology 200, 103-123. https://doi.org/10.1016/S0025-
580 3227(03)00179-8.

581 De Falco, G., Antonioli, F., Fontolan, G., Lo Presti, V., Simeone, S., Tonielli, R., 2015. Early cementation
582 and accommodation space dictate the evolution of an overstepping barrier system during the Holocene.
583 Marine Geology 369, 52-66. https://doi.org/10.1016/j.margeo.2015.08.002

584 Del Grande, C., Gabbianelli, G., Fontolan, G., 2001. Short-term evolutionary model of coastal spits, an
585 example from Goro Lagoon (Po Delta Italy). 21st IAS Meeting of Sedimentology Abstracts, Abstract T3-
586 267, Davos, Switzerland, 3-5 September 2001.

587 Elliott, T., 1986a. Deltas. In: Reading, H.G. (Ed.), Sedimentary Environments and Facies. Blackwell
588 Scientific Publications, Oxford: pp. 113-154.

589 Elliott, T., 1986b. Siliciclastic shorelines. In: Reading, H.G. (Ed.), Sedimentary Environments and Facies.
590 Blackwell Scientific Publications, Oxford: pp. 155-188.

591 Falqués, A., Ribas, F., Calvete, D., 2018. Rhythmic shoreline features. Available from
592 http://www.coastalwiki.org/wiki/Rhythmic_shoreline_features (accessed on 18.06.2019)

593 Falqués, A., Ribas, F., Idier, D., Arriaga, J., 2017. Formation mechanisms for self-organized kilometer-
594 scale shoreline sand waves. Journal of Geophysical Research Earth Surface 122, 1121–1138.
595 https://doi.org/10.1002/2016JF003964

596 FitzGerald, D.M., 1988. Shoreline erosional-depositional processes associated with tidal inlets. In:
597 Aubrey, D.G. and Weishar, L. (Eds.), Hydrodynamics and Sediment Dynamics of Tidal Inlets, Lecture
598 Notes on Coastal and Estuarine Studies 29, 186-225.

599 FitzGerald, D.M., Hein, C., Hughes, Z., Kulp, M., Georgiou, I., Miner, M.. 2018 Runaway barrier island
600 transgression concept: global case studies. In Springer International Publishing AG 2018 3 Moore, L.J.,
601 Murray, A.B. (eds.), Barrier Dynamics and Response to Changing Climate, pp 3-56.
602 https://doi.org/10.1007/978-3-319-68086-6_1

603 Fontolan, G., Covelli, S., Bezzi, A., Tesolin, V., Simeoni, U., 2000. Stratigrafia dei depositi recenti della
604 Sacca di Goro. Studi Costieri 2, 65-79.

605 Forde, T.C., Nedimović, M.R.,Gibling, M.R., Forbes, D.L., 2015. Coastal evolution over the past 3000 years
606 at Conrads Beach, Nova Scotia: the influence of local sediment supply on a paraglacial transgressive
607 system. Estuaries and Coasts 39: 363-384. https://doi.org/10.1007/s12237-015-0016-6

608 Fruergaard, M., Møller, I., Johannessen, P.N., Nielsen, L.H., Andersen T.J., Nielsen, L., Sander, L., Pejrup
609 M., 2015. Stratigraphy, evolution, and controls of a Holocene transgressive–regressive barrier island

610 under changing sea level: Danish North Sea coast. Journal of Sedimentary Research 85, 820–844.
611 http://dx.doi.org/10.2110/jsr.2015.53

612 Galloway, W.E., 1975. Process framework for describing the morphologic and stratigraphic evolution of
613 deltaic depositional systems. In Broussard, M.L. (Ed.), Deltas: Models for Exploration, Houston geological
614 Society, Houston, pp.87-98.

615 Garrison, J.R., Williams, J., Potter Miller S., Weber E.T., McMechan, G., Zeng, X., 2010. Ground-
616 penetrating radar study of North Padre Island: implications for barrier island internal architecture,
617 model for growth of progradational microtidal barrier islands, and Gulf of Mexico sea-level cyclicity.
618 Journal of Sedimentary Research 80 (4), 303-319. http://dx.doi.org/10.2110/jsr.2010.034

619 Gerdes, G., 2007. Structures left by modern microbial mats in their host sediments. In: Schieber, J., Bose,
620 P.K., Eriksson, P.G., Banerjee, S., Sarkar, S., Altermann W., Catuneau, O. (Eds.), Atlas of microbial mat
621 features preserved within the clastic rock record. Elsevier, pp. 5-38.

622 González-Villanueva, R., Pérez-Arlucea, M., Costas, S., Bao, R., Otero, X.L., Goble, R.J., 2015. 8000 years
623 of environmental evolution of barrier–lagoon systems emplaced in coastal embayments (NW Iberia).
624 The Holocene 25(11), 1786-1801. https://doi.org/10.1177/0959683615591351.

625 Got, H., Aloïsi, J.C., Monaco, A., 1985. Sedimentary processes in Mediterranean deltas and shelves. In:
626 Stanley, S.J., Wezel, F.C. (Eds.) Geological evolution of the Mediterranean basin. Springer, New York: pp.
627 355-376.

628 Hayes, M.O., Ruby, C.H., 1994. Barriers of Pacific Alaska. In: Davis, R.A. (Ed.), Geology of Holocene
629 barrier island systems. Springer, Berlin, Heidelberg: pp. 395-433. https://doi.org/10.1007/978-3-642-
630 78360-9_9

631 Héquette, A., Ruz, M.H., 1991. Spit and barrier island migration in the Southestern Canadian Beaufort
632 Sea. Journal of Coastal Research 7(3), 677-698.

633 Hine, A.C., 1979. Mechanism of berm development and resulting beach growth along a barrier spit
634 complex. Sedimentology 26, 333-351. https://doi.org/10.1111/j.1365-3091.1979.tb00913.x

635 Hein, C, J., FitzGerald, D.M., Cleary, W.J., Albernaz, M.B., de Menezes, J.T., Da Fontoura Klein, A.H., 2013.
636 Evidence for a transgressive barrier within a regressive strandplain system: Implications for complex
637 coastal response to environmental change. Sedimentology 60, 469 – 502.
638 https://doi.org/10.1111/j.1365-3091.2012.01348.x

639 Jensen, S.G., Aagaard, T., Baldock, T.E., Kroon, A., Hughes, M., 2009. Berm formation and dynamics on a
640 gently sloping beach; the effect of water level and swash overtopping. Earth Surface Processes and
641 Landforms 34, 1533-1546. https://doi.org/10.1002/esp.1845.

642 Leatherman, S.P., Williams, A.T., Fisher, J.S., 1977. Overwash sedimentation associated with a large scale
643 northeastern. Marine Geology 24, 109-121. https://doi.org/10.1016/0025-3227(77)90004-4

644 Manzo, C., Braga, F., Zaggia, L., Brando, V.E., Giardino C., Bresciani, M., Bassani, C., 2018. Spatio-
645 temporal analysis of prodelta dynamics by means of new satellite generation: the case of Po river by
646 Landsat-8 data. International Journal of Applied Earth Observation and Geoinformation 66, 210-225.
647 https://doi.org/10.1016/j.jag.2017.11.012

648 McBride, R.A., Byrnes, M.R., 1997. Regional variations in shore response along barrier island systems of
649 the Mississippi river delta plain: historical change and future prediction. Journal of Coastal Research 13
650 (3), 628-655.

McBride R.A., Byrnes, M.R., Hiland, M.W., 1995. Geomorphic response-type model for barrier coastlines: a regional perspective. Marine Geology 126, 143-159. https://doi.org/10.1016/0025-3227(95)00070-F.

Morton, R.A., 1994. Texas barriers. In: Davis, R.A. (Ed.), Geology of Holocene barrier island systems. Springer, Berlin, Heidelberg: pp. 75-114. https://doi.org/10.1007/978-3-642-78360-9_3

Niedoroda, A.W.,Tanner, W.F., 1970. Preliminary study on transverse bars. Marine Geology 9, 41–62. https://doi.org/10.1016/0025-3227(70)90079-4

Nittrouer, C.A., Miserocchi, S., Trincardi, F., 2004. The PASTA Project. Investigation of Po and Apennine Sediment Transport and Accumulation. Oceanography 17(4): 46–57. https://doi.org/10.5670/oceanog.2004.03.

Orford, J.D., Carter, R.W.G., 1982. Crestal overtop and washover sedimentation on a fringing sandy gravel barrier coast, Carnsore Point, Southeastern Ireland. Journal of Sedimentary Petrology 52, 265-278. https://doi.org/10.1306/212F7F2C-2B24-11D7-8648000102C1865D

Otvos, E.G., 2000. Beach ridges – definitions and significance. Geomorphology 32, 83-108. https://doi.org/10.1016/S0169-555X(99)00075-6.

Otvos, E.G., 2018. Coastal barriers, northern Gulf-Last Eustatic Cycle; genetic categories and develo pmental contrasts. A Review. Quaternary Science Reviews 193, 212-243. https://doi.org/10.1016/j.quascirev.2018.04.001

Pellón, E., Garnier, R., Medina, R., 2014. Intertidal finger bars at El Puntal, Bay of Santander, Spain: observation and forcing analysis. Earth Surface Dynamics 2, 349-361. https://doi.org/10.5194/esurf-2-349-2014

671 Raff, J.L., Shawler, J.L., Ciarletta, D.J., Hein, E.A., Lorenzo-Trueba, J., Hein, C.J., 2018. Insights into barrier-
672 island stability derived from transgressive/regressive state changes of Parramore Island, Virginia. Marine
673 Geology 403, 1-19. https://doi.org/10.1016/j.margeo.2018.04.007

674 Reineck, H.E., Singh, I.B., 1980. Depositional Sedimentary Environments. Springer-Verlag, New York, 549.
675 https://doi.org/10.1007/978-3-642-81498-3

676 Ritchie, A. C., Warrick, J. A., East, A. E., Magirl, C. S., Stevens, A. W., Bountry, J. A., Randle, T. J., Curran, C.
677 A., Hilldale, R. C., Duda, J. J., Miller, I. M., Pess, G. R., Foley, M. M., McCoy, R., Ogston, A. S., 2018.
678 Morphodynamic evolution following sediment release from the world's largest dam removal. Nature
679 Scientific Reports 8, 13279 https://doi.org/10.1038/s41598-018-30817-8

680 Rodriguez, A.B., Yu, W., Theuerkauf, E.J., 2018. Abrupt increase in washover deposition along a
681 transgressive barrier island during the late nineteenth century acceleration in sea-level rise. In: Moore,
682 L., Murray, A., (Eds.), Barrier Dynamics and Response to Changing Climate. Springer, Cham.
683 https://doi.org/10.1007/978-3-319-68086-6_4

684 Rubin, Z.K., Kondolf, G.M., Carling, P.A., 2015. Anticipated geomorphic impacts from Mekong basin dam
685 construction. International Journal of River Basin Management 13, 105-121.
686 https://doi.org/10.1080/15715124.2014.981193

687 Ruol, P., Martinelli, L., Favaretto, C., 2018. Vulnerability analysis of Venetian littoral and adopted
688 mitigation strategy. Water, 10, 984. https://doi.org/10.3390/w10080984

689 Sanders, J.E., Kumar, N., 1975. Evidence of shoreface retreat and in-place “drowning” during Holocene
690 submergence of barriers, shelf of Fire Island, New York. Geological Society of America Bulletin 86, 65-76.

691 Schwartz, R.K., 1982. Bedform and stratification characteristics of same modern small-scale washover
692 sand bodies. Sedimentology 29, 835-849.

693 Simeoni, U., (Ed.) 2000. La Sacca di Goro. Studi Costieri 2, pp. 239.

694 Simeoni, U., Corbau, C., 2009. A review of the Delta Po evolution (Italy) related to climatic changes and
695 human impacts. Geomorphology 107, 64–71. https://doi.org/10.1016/j.geomorph.2008.11.004

696 Simeoni, U., Fontolan, G., Dal Cin, R., Calderoni, G., Zamariolo, A, 2000. Dinamica sedimentaria dell'area
697 di Goro (delta del Po). Studi costieri 2, 139-151.

698 Simeoni, U., Fontolan, G., Tessari, U., Corbau, C., 2007. Domains of spit evolution in the Goro area, Po
699 Delta, Italy. Geomorphology 86, 332-348. https://doi.org/10.1016/j.geomorph.2006.09.006

700 Suter, J.R., 1994. Deltaic coasts. In: Carter, R.W.G. and Woodroffe, C.D. (Eds.), Coastal evolution: late
701 Quaternary shoreline morphodynamics. Cambridge University Press, Cambridge, pp. 87-120.

702 Timmons, E.A., Rodriguez, A.B., Christopher, R.M., DeWitt R., 2010. Transition of a regressive to a
703 transgressive barrier island due to back-barrier erosion, increased storminess, and low sediment supply:
704 Bogue Banks, North Carolina, USA. Marine Geology 278, 100–114.
705 http://doi.org/10.1016/j.margeo.2010.09.006

706 Welch, A.C., Nicholls, R.J., Lázár, A.N., 2017. Evolving deltas: Coevolution with engineered interventions.
707 Elementa Science of the Anthropocene 5, p. 49. http://doi.org/10.1525/elementa.128

- The deltaic barrier spit system of Goro is prograding during 1955-2000.
- Development of contiguous depositional environments occurs at human scale.
- Detailed core stratigraphy and historical aerial photos are coupled.
- X-rays improve recognition of sedimentary structures and events.
- The anthropic interaction leaves recognizable signatures in the sedimentary record.